

NBSIR 79-1601

NBS  
PUBLICATIONS



# THE EFFECTS OF RESISTIVE LOADING ON TEM HORNS

---

Motohisa Kanda

Electromagnetic Fields Division  
National Engineering Laboratory  
National Bureau of Standards  
Boulder, Colorado 80303

August 1979

QC  
100  
J56  
79-1601  
979  
.2



JAN 31 1980

NBSIR 79-1601

9 4 2

79-1601  
102

# THE EFFECTS OF RESISTIVE LOADING ON TEM HORNS

---

Motohisa Kanda

Electromagnetic Fields Division  
National Engineering Laboratory  
National Bureau of Standards  
Boulder, Colorado 80303

August 1979



---

U.S. DEPARTMENT OF COMMERCE, Juanita M. Kreps, Secretary

Sidney Harman, Under Secretary

Jordan J. Baruch, Assistant Secretary for Science and Technology

NATIONAL BUREAU OF STANDARDS, Ernest Ambler, Director



## Contents

	<u>Page</u>
1. INTRODUCTION	1
2. THEORETICAL CONSIDERATIONS	2
2.1 A Resistively Loaded "TEM" Horn	2
2.2 Conductive TEM Horns	6
3. CHARACTERISTICS OF RESISTIVELY LOADED "TEM" HORNS	10
3.1 Loading Profile	10
3.2 Current Distribution	10
3.3 Driving-Point Impedance	11
3.4 Reflection Coefficient	11
3.5 Radiation Power Pattern	11
4. FREQUENCY DOMAIN RESULTS	12
5. TIME-DOMAIN RESULTS	13
6. CONCLUSION	14
7. References	15
Figure Captions	16

# The Effects of Resistive Loading of "TEM" Horns

Motohisa Kanda

Electromagnetic Fields Division

National Bureau of Standards

Boulder, Colorado 80303

For directional reception or transmission of picosecond pulses with minimal distortion, a short transverse electromagnetic (TEM) horn with continuously tapered resistive loading was developed and found to be broadband and nondispersive with a low VSWR. The receiving transient response of the resistively loaded "TEM" horn indicates that the shape of a 70-ps impulse is well preserved. The theoretical analyses using the method of moments and the fast Fourier transform (FFT) technique were performed and agreed well with time-domain measurements.

Key words: Broadband; directivity; effective length; FFT; method of moments; nondispersive; picosecond pulse; resistive loading; TEM horn; transfer function; transient.

## 1. INTRODUCTION

Recent study related to electromagnetic pulse (EMP) phenomena has focused strong attention on the subject of transient electromagnetic (EM) fields. Antenna structures able to preserve the time-domain waveform of EMP must be inherently broadband and nondispersive. One such antenna, which has been successfully fabricated, is a dipole with continuously tapered resistive loading [1,2].

In an effort to attain increased directivity or increased antenna gain for a broadband and nondispersive antenna, many researchers have considered a transverse electromagnetic (TEM) horn, which is a two-conductor, end-fire traveling-wave structure. If the flare angle and the plate widths of a TEM horn are properly chosen so that a constant, characteristic impedance can be maintained, the horn will guide an essentially TEM mode into free space. Thus, a TEM horn can be considered as a transition section which transfers EM energy from a transmission line to free space. In order to achieve a "smooth" transition, i.e., a transition with low reflection, the length of a conventional conductive TEM horn has to be at least one-half wavelength long at the lowest frequency of interest. This means that, if the lowest frequency of interest is 100 MHz, a TEM horn may be as long as 1.5 m, which is too long to be practical.

The Cornell Aeronautical Laboratory (CAL) designed a TEM horn with nonuniform-line matching from  $50 \Omega$  at the antenna throat to  $377 \Omega$  at the aperture. The nonuniform-line matching was achieved by forming the TEM horn plates empirically into tear-drop shapes. A small resistance card termination was placed at the tip of the aperture to provide adequate current attenuation for a traveling wave. With these empirical modifications, the length of the TEM horn was reduced to 1 m with a reasonable reflection coefficient (less than 0.48) for the frequency range of 100 MHz to 2 GHz.

In this paper, a "TEM" horn with continuously tapered resistive loading is considered for the purpose of developing a relatively short, broadband and nondispersive antenna with high directivity. One-dimensional, theoretical analysis for a resistively loaded "TEM" horn using the method of moments [3] has been performed in the frequency domain. Using the fast Fourier transform

(FFT) technique then allows the determination of transient radiated EM fields for a known input pulse waveform. Comparison between theory and time-domain measurements is also given in this paper.

## 2. THEORETICAL CONSIDERATIONS

In this section, the theoretical considerations for a one-dimensional model of a resistively loaded "TEM" horn, as shown in figure 1, are given first. A one-dimensional analysis simplifies the mathematics involved, yet gives good physical insight for evaluating the effects of resistive loading on a TEM horn.

To analyze a conductive TEM horn, a biconical antenna model given in figure 2 is used. By adjusting the apex angle and the lengths of the cones, this model gives good physical understanding for analyzing conductive TEM horns.

### 2.1 A Resistively Loaded "TEM" Horn

Because of the presence of loss in TEM horn plates, the field patterns for EM waves propagating between lossy plates deviate from a pure TEM mode. Because a resistively loaded "TEM" horn cannot support a pure TEM mode, the term "TEM" horn may not be truly appropriate but will be used throughout this paper.

If there are abrupt changes in the characteristics of the boundary (i.e., air to lossy TEM horn plate), the problem can be solved by finding general solutions for each of the regions and evaluating unknown constants by satisfying the boundary conditions across plate interfaces. A transcendental matrix equation derived by matching the field across plate interface is not, however, expected to be easy to solve in general cases. For this reason, the analysis used in the paper is a one-dimensional model given in figure 1, which ignores any transverse current components on the lossy plates. When the horn angle and the plate widths are so chosen that they vary smoothly, it is a reasonably good assumption to neglect transversal components of current on the lossy plates. The shape for horn plates in the study is, therefore, chosen to be triangular.

Using the one-dimensional model which neglects any transverse components of current on the lossy plate, we calculate numerically the longitudinal

component of the current by using the method of moments. In this paper, we review briefly a general theoretical development for a one-dimensional, resistively loaded antenna structure, which can be bent and can have step discontinuities in radius. More detailed discussion on the theory is given elsewhere [3,4].

Figure 1 shows a typical one-dimensional structure of a TEM horn modeled by straight sections with a bend at a junction. Using a one-dimensional model, the current is assumed to be uniform perpendicular to the figure and to flow in one direction on each plate. Then, the incident electrical field  $E_{inc}$  associated with the current  $I$  and the charge density  $\rho$  on a one-dimensional plate are given in terms of usual vector and scalar potentials  $\vec{A}$  and  $\phi$ :

$$\vec{E}_{inc} = -j\omega\vec{A} - \nabla\phi, \quad (1)$$

$$\vec{A} = \frac{\mu}{4\pi} \int_C I(s') \vec{U}(s') \frac{e^{-jkR}}{R} ds', \quad (2)$$

and

$$\phi = \frac{1}{4\pi} \int_C \rho(s') \frac{e^{-jkR}}{R} ds', \quad (3)$$

where  $R$  is defined to be:

$$R = \sqrt{|r-r'(s')|^2 + a^2(s')}. \quad (4)$$

One-dimensional charge density  $\rho(s)$  is related to the current  $I(s)$  through the equation of continuity:

$$\rho(s) = \frac{-1}{j\omega} \frac{dI(s)}{ds}. \quad (5)$$

The unit direction vector  $\vec{U}$ , which is parallel to the axis of each segment, is defined as:

$$\vec{U}_{n+\frac{1}{2}} = \frac{\vec{r}_{n+1} - \vec{r}_n}{|\vec{r}_{n+1} - \vec{r}_n|} \cdot \quad (6)$$

Using the pulse-testing function, expanding the current in pulses, and applying a finite difference approximation to compute charge density  $\rho$ , we can rearrange eq (1) in terms of the usual impedance matrix  $Z_{mn}$  associated with the current and voltage matrix  $I_n$  and  $V_m$ , i.e.,

$$\sum_{n=1}^N I_n Z_{mn} = V_m \cdot \quad (7)$$

The matrix element  $Z_{mn}$  associated with the  $n$ th current at the observation  $s_m$  is given by [4]:

$$\begin{aligned} Z_{mn} = & \frac{-1}{4\pi j \omega \epsilon} \left[ k^2 (\vec{r}_{m+\frac{1}{2}} - \vec{r}_{m-\frac{1}{2}}) \cdot (\vec{S}_{n+\frac{1}{2}} \psi_{m,n,n+\frac{1}{2}} + \vec{S}_{n-\frac{1}{2}} \psi_{m,n-\frac{1}{2},n}) \right. \\ & \left. - \frac{\psi_{m+\frac{1}{2},n,n+1}}{s_{n+1} - s_n} + \frac{\psi_{m+\frac{1}{2},n-1,n}}{s_n - s_{n-1}} + \frac{\psi_{m-\frac{1}{2},n,n+1}}{s_{n+1} - s_n} - \frac{\psi_{m-\frac{1}{2},n-1,n}}{s_n - s_{n-1}} \right] \\ & + Z(s_m) (s_{m+\frac{1}{2}} - s_{m-\frac{1}{2}}), \end{aligned} \quad (8)$$

where  $Z(s_m)$  is the internal resistance per unit length due to resistive loading. Both the vector and scalar potential terms involve the integral of the form:

$$\Psi_{m,\mu,\nu} = \int_{s_\mu}^{s_\nu} \frac{e^{-jkR_m}}{R_m} ds', \quad (9)$$

where

$$R_m = \sqrt{|\vec{r}_m - \vec{r}'(s')|^2 + a^2(s')}. \quad (10)$$

The matrix element  $V_m$  is simply given by:

$$V_m = E_m^{\text{inc}}(s_m) \cdot (V_{m+\frac{1}{2}} - V_{m-\frac{1}{2}}). \quad (11)$$

The resistive loading profile  $Z(s)$  in ohms per meter of a "TEM" horn is expressed as:

$$Z(s) = \frac{Z_0}{1 - \frac{s}{L}} \Omega/\text{m}, \quad 0 \leq s \leq L, \quad (12)$$

where  $Z_0$  is the resistance per unit length ( $\Omega/\text{m}$ ) at the driving point, and  $L$  is the length of the "TEM" horn. Equation (12) predicts that the resistive loading of the "TEM" horn increases continuously from the value  $Z_0$  ( $\Omega/\text{m}$ ) at the driving point to infinity at the end of the "TEM" horn. The choice of this particular resistive loading profile, which enables a TEM horn to handle extremely wide bandwidth signals without dispersion distortion, has been given by many researchers [5,6,7,8] as well as by the author [1,2]. In essence, there exists a critical value for  $Z_0$ , for which a "TEM" horn can sustain a traveling-wave current from the driving point toward the end of the "TEM" horn. A traveling-wave structure supporting TEM mode propagation is essential for transmitting and receiving a signal with large instantaneous bandwidth without serious pulse broadening or wide angle sidelobes.

Once the current distribution of the resistively loaded "TEM" horn is determined, the effective length  $h_e(f)$  of the antenna can be calculated from the moment of its current distribution divided by the driving-point current, i.e.:

$$h_e(f) = \frac{1}{I_z(0)} \int I_z(z') dz'. \quad (13)$$

The effective length and the driving-point impedance of the antenna are required later to evaluate its transfer function.

A formal solution to the resistively loaded "TEM" horn problem can be formulated by modeling solid plate surfaces with loaded wire grids or meshes. This extends the one-dimensional problem to a two- or three-dimensional problem by taking into account the transverse current components on horn plates. The moment method technique will give a reasonable solution in the frequency range in which each surface is smaller than a few square

wavelengths. Above those frequencies, the moment method unfortunately needs many loaded wire segments and therefore requires many unknown currents to accurately model a solid surface. In this case, perhaps the geometrical theory of diffraction (GTD) technique would provide more efficient solutions to this problem. These techniques will be pursued for better understanding of a resistively loaded "TEM" horn.

In the present study, the one-dimensional theoretical analysis for the resistively loaded "TEM" horn using the method of moments [3] has been performed in the frequency domain. Using the FFT then allows the determination of transient characteristics of the antenna.

## 2.2 Conductive TEM Horns

In a previous paper by the author [9,10], a simple theoretical model was developed using the assumed aperture field. In this model the horn flare angle and the plate widths are chosen so that the TEM horn guides only the TEM mode by maintaining a constant impedance. If the edge diffraction effect and fringe fields are neglected, the aperture field of the TEM horn is assumed to be a linearly polarized, spherical field. Once an aperture field is established, the radiated EM field at any distance can be evaluated using the plane-wave spectrum analysis technique.

As discussed in [9,10], a number of major limitations of the simplified theoretical model still remain, although some useful engineering design concepts were obtained. For example, the assumption that a TEM mode is basically guided from the throat to the aperture by the nondispersive TEM horn is highly questionable. Particularly at the high frequency range of the spectrum, above 1 GHz for example, the aperture field may be quite different from a basic TEM mode due to higher modes. Even at the lower frequency ranges, below 1 GHz for example, the magnitude of the TEM mode at the aperture may not remain constant due to a high reflection coefficient, e.g., 0.98 at 100 MHz.

In an effort to treat these aspects more rigorously, a formal solution to the TEM horn problem using a vector integral equation technique was proposed. Using the equivalence principle [11], the electric field  $\vec{E}$  in the free space generated by an unknown set of electric currents  $\vec{J}$  on the TEM horn plates is:

$$\vec{E} = -\nabla \times \vec{F} - j\omega\mu\vec{A} + \frac{1}{j\omega\epsilon} \nabla(\nabla \cdot \vec{A}), \quad (14)$$

where the electric vector potential  $\vec{F}$  is given in terms of the known excitation equivalent magnetic current by  $\vec{M}$ :

$$\vec{F} = \frac{1}{4\pi} \iint_{\text{source}} \vec{M} \frac{e^{-jkR}}{R} ds, \quad (15)$$

and the magnetic vector potential  $\vec{A}$  is given in terms of the unknown current  $\vec{J}$  on the TEM horn plates by:

$$\vec{A} = \frac{1}{4\pi} \iint_{\text{plates}} \vec{J} \frac{e^{-jkR}}{R} ds, \quad (16)$$

with  $R = |r-r'|$ .

Boundary conditions are such that the tangential electric field at the TEM horn plates is zero, i.e.:

$$\vec{n} \times \vec{E} = 0 \quad \left| \quad \text{on the plates.} \quad (17)$$

Substituting eqs (14), (15), and (16) into eq (17) gives:

$$\begin{aligned} \vec{n} \times \left( -\nabla \times \frac{1}{4\pi} \iint \vec{M} \frac{e^{-jkR}}{R} ds \right) + \vec{n} \times \left[ -\frac{j\omega\mu}{4} \iint \vec{J} \frac{e^{-jkR}}{R} ds \right. \\ \left. + \frac{1}{j\omega\epsilon} \nabla(\nabla \times \frac{1}{4\pi} \iint \vec{J} \frac{e^{-jkR}}{R} ds) \right] = 0 \quad \left| \quad \text{on the plates.} \quad (18) \end{aligned}$$

The above electric field integral equation may be solved for the unknown  $\vec{J}$ . Once  $\vec{J}$  is determined, the other EM fields everywhere may be determined by use of eqs (14), (15), and (16).

The derivation of the electric field integral equation given in eq (18) is complete and straightforward. The solution may also be obvious using the method of moments technique. The horn plates are divided into small patches.

After the vector integral equation given in eq (18) is decomposed into appropriate coupled scalar integral equations, two orthogonal components of current  $\vec{J}$  with two unknown constants over each patch must be forced to satisfy the boundary condition. Although the matrix formulations of the problem are quite straightforward, their solution can get extremely formidable, particularly at higher frequencies where each patch has to be divided into smaller ones compared to wavelength. Although some symmetry arguments may be used to keep the matrix sizes tractable, there is no easy way out except to perform a very large matrix computation. In addition, because the FFT is used to obtain the transient characteristics of the TEM horn, the above electric field integral equation has to be solved for many frequency points, e.g., on the order of one thousand from 10 MHz to several GHz. This is a very expensive process.

In this paper, a simple model, modified from one used in previous papers by the author [9,10], is adopted to analyze a conductive TEM horn. The model used is a biconical antenna structure, where the apex angle and the length of a bicone are adjusted to fit a TEM horn. The biconical model of a conducting TEM horn is shown in figure 2. A knowledge of both the driving-point impedance and the effective length of the antenna for the frequency range over which the spectrum of the excitation has significant amplitude is required to discuss quantitatively the transient response of a transmitting and receiving TEM horn using the FFT technique.

The effective length  $h_e(f)$  and the driving-point impedance  $Z_0(f)$  of a wide-angle conical antenna, studied by many workers [12] as well as by the author [9,10], are given respectively by:

$$h_e(f) = \frac{1}{k^2 \ell \left(1 + \frac{\beta}{\alpha}\right)} \left( \frac{\beta}{\alpha} e^{jk\ell} - e^{-jk\ell} \right) \tag{19}$$

$$\sum_{n=1}^{\infty} P_n(\cos \theta_0) P_n'(0) \left( \frac{2n+1}{n^2+n} \right) \frac{j^{n+1}}{h_{n-1}^{(2)}(k\ell) - \frac{n}{ka} h_n^{(2)}(k\ell)}$$

and

$$Z_0(f) = Z_c \left( \frac{1 - \frac{\beta}{\alpha}}{1 + \frac{\beta}{\alpha}} \right). \quad (20)$$

The symbols have the following meanings:

$\ell$  is the length of the antenna,

$P_n(\cos \theta)$  is the Legendre polynomial of order  $n$ ,

$h_n^{(2)}(k\ell)$  is the spherical Hankel function of the second kind,

$$Z_c = 60\ell n \cot \frac{\theta_0}{2}, \quad (21)$$

$$\frac{\beta}{\alpha} = e^{-j2ka} \left\{ \frac{1 + j \frac{60}{Z_c} \sum_{n=1}^{\infty} \frac{2n+1}{n(n+1)} \left( P_n(\cos \theta_0) \right)^2 \zeta_n(k\ell)}{-1 + j \frac{60}{Z_c} \sum_{n=1}^{\infty} \frac{2n+1}{n(n+1)} \left( P_n(\cos \theta_0) \right)^2 \zeta_n(k\ell)} \right\}, \quad (22)$$

and

$$\zeta_n(ka) = \frac{h_n^{(2)}(k\ell)}{h_{n-1}^{(2)}(k\ell) - \frac{n}{ka} h_n^{(2)}(k\ell)}. \quad (23)$$

Then the far-field electric field is given by:

$$E(f) = j \frac{60}{Z_0(f) + Z_g} F(f) \frac{e^{-jkr}}{r}, \quad (24)$$

where the field characteristic  $F(f)$  is related to the effective length  $h_e(f)$  through the Rayleigh-Carson reciprocity theorem [13]:

$$F(f) = kh_e(f). \quad (25)$$

### 3. CHARACTERISTICS OF RESISTIVELY LOADED "TEM" HORNS

#### 3.1 Loading Profile

In the present study, the one-dimensional theoretical analysis for a triangularly shaped "TEM" horn with resistive loading has been performed to solve for the current distribution using the method of moments. The physical dimensions of the TEM horn are shown in figure 3.

If  $Z_0$  in eq (12) is chosen to be about  $14 \Omega/m$ , then a 36-cm long "TEM" horn can sustain a traveling-wave current along the antenna for the frequency range of 100 MHz to 8 GHz. When  $Z_0$  is lower than  $14 \Omega/m$ , the current distributions along the antenna are similar to standing waves. On the other hand, when  $Z_0$  is much higher than  $14 \Omega/m$ , the current distribution is overdamped, and the radiation efficiency of the antenna is expected to be very low because the antenna is acting like a load termination.

Several resistively loaded "TEM" horns have been made by sputtering copper on polycarbonate substrates ( $\epsilon_r \approx 3$ ). The required resistive-loading profile was obtained by moving the substrate through a stationary mask.

#### 3.2 Current Distribution

The current distributions on the resistively loaded, 36-cm long "TEM" horn are calculated numerically using the method of moments for the frequency range of 10 MHz to 5 GHz. The discussion of the numerical technique used to calculate the current distribution on the resistively loaded "TEM" was given briefly in section 2.1.

The current distribution at frequencies above 100 MHz is a traveling wave, whereas that below 100 MHz exhibits some standing-wave component due to a reflection from the end. Figure 4 shows the current distribution at 1 GHz along with the experimental results. The current distribution measurement was made using a 1-cm diameter loop with a beam lead Schottky diode. The discrepancy between theoretical and experimental results is mainly due to experimental difficulties encountered in measuring current distribution using the electrically small loop antenna.

### 3.3 Driving-Point Impedance

Figure 5 shows the driving-point resistance and reactance obtained by the method of moments along with the experimental results. The experimental results were obtained using an automatic network analyzer. The impedance of the resistively loaded "TEM" horn typically has a resistance of about 70  $\Omega$  and a capacitance of about 27 pF in a series configuration.

### 3.4 Reflection Coefficient

The input reflection coefficient of the 36-cm long resistively loaded "TEM" horn is shown in figure 6. The reflection coefficient typically stays below 0.5 for the frequency range from 100 MHz to 8 GHz as shown in this figure. For comparison, the reflection coefficients of a 36-cm long conducting TEM horn and a 1-m long CAL TEM horn are also shown in figure 7. This figure indicates that the reflection coefficient of the TEM horn has been significantly improved through resistive loading, and that the reflection coefficient of the 36-cm long resistively loaded "TEM" horn is comparable to that of a 1-m long CAL TEM horn. On the other hand, the reflection coefficient of a conducting TEM horn is very high, particularly at the low-frequency range (0.98 at 100 MHz), and shows an oscillatory nature above 1 GHz due to multiple reflections between the throat and the aperture as shown in figure 7.

### 3.5 Radiation Power Pattern

To obtain the far-field radiation power pattern of the resistively loaded "TEM" horn, it is assumed that the current flows in the direction of the axis of the antenna, and that transverse components of current are ignored. Once the current distribution of the antenna is determined, the far-field radiation power pattern in the E plane ( $E_{\parallel}^r$ ) is given by:

$$\begin{aligned}
E_{\parallel}^r(\theta) &= j\omega \sin(\theta - \Delta/2) \frac{\mu_0 e^{-jkr}}{4\pi r} \int I_z(z') e^{-jkz' \cos(\theta - \Delta/2)} dz' \\
&\quad - j\omega \sin(\theta + \Delta/2) \frac{\mu_0 e^{-jkr}}{4\pi r} \int I_z(z') e^{-jkz' \cos(\theta + \Delta/2)} dz'.
\end{aligned} \tag{26}$$

The far-field radiation power pattern in the H plane ( $E_{\perp}^r$ ) is given by:

$$E_{\perp}^r(\theta) = 2 \sin(\alpha) E_{\parallel}^r(\theta), \tag{27}$$

where

$$\sin(\alpha) = \frac{\sin(\Delta)}{\sqrt{1 - \cos^2 \theta \cdot \cos^2(\Delta)}}. \tag{28}$$

The geometry considered is shown in figure 8. The theoretical results of far-field power patterns in the E and H planes are shown respectively in figures 9 and 10.

Experiments to measure radiation power patterns of the antenna in both the E and H planes were performed in an anechoic room using a standard horn as a transmitting antenna. The results are also shown in figures 9 and 10. It is found from these figures that the half-power beamwidths of the antenna are typically  $100^\circ$  in both E and H planes at 1 GHz. The directivity of the antenna is then roughly estimated to be about 6 dB at 1 GHz.

#### 4. FREQUENCY DOMAIN RESULTS

The frequency-domain representation of the receiving transfer function  $S_r(f)$  of the resistively loaded "TEM" horn is given by:

$$S_r(f) = \frac{V_L(f)}{E_{inc}(f)} = \frac{-h_e(f) Z_L(f)}{Z_0(f) + Z_L(f)}, \tag{29}$$

where  $V_L(f)$  is the load voltage (V),  $E_{inc}$  is the normal incident electric field (V/m),  $h_e(f)$  is the effective length of the antenna (m),  $Z_0(f)$  is the driving-point impedance of the antenna ( $\Omega$ ), and  $Z_L(f)$  is the load impedance ( $\Omega$ ).

Using the effective length of the antenna (which is defined as the moment of its current distribution derived from the input current) and the driving-point impedance of the antenna, we calculate the frequency-domain representation of the receiving transfer function of the antenna using eq (29). The receiving transfer functions of the resistively loaded "TEM" horn and the conductive TEM horn are shown in figures 11 and 12, respectively.

Experiments were performed using a time-domain antenna range with a time-domain automatic network analyzer. The experimental results of the receiving transfer function of the resistively loaded "TEM" horn and that of a conductive TEM horn of the same size are also shown in figures 11 and 12, respectively.

The theoretical and experimental results for the receiving transfer function of the resistively loaded "TEM" horn agree well. The receiving transfer function of the antenna is flat to within  $\pm 3$  dB from 20 MHz to 7 GHz. On the other hand, the experimental results of the transfer function for a conducting TEM horn indicate that there are strong resonances in the horn and that its transfer function is not nearly as flat as that of the resistively loaded "TEM" horn.

## 5. TIME-DOMAIN RESULTS

Once frequency-domain solutions are determined, transient fields for a known input waveform can be found using the FFT technique. The experiments were performed using a time-domain antenna range with a time-domain automatic network analyzer. The impulse generator generates extremely narrow (70 ps) duration impulses with flat spectrum amplitudes greater than 60 dB V/MHz up to 5 GHz, as shown in figure 13. 70 ps was used both as a driving voltage for the investigation of transmitting transient responses and as an incident impulse field for the investigation of receiving transient responses. The theoretical and experimental transient characteristics of receiving and transmitting responses for the resistively loaded "TEM" horn are shown in figure 14. As this figure indicates, there is an agreement between theory and experimental results of the receiving and transmitting responses.

## 6. CONCLUSION

For directional reception or transmission of picosecond pulses with minimal distortion, a short "TEM" horn with continuously tapered, resistive loading was developed, and was found to be broadband and nondispersive with a low VSWR. The receiving transient response of the resistively loaded "TEM" horn indicates that the shape of 70 ps is well preserved. Theoretical computations using the method of moments and the FFT technique were performed and agreed well with time-domain measurements. The short "TEM" horn with continuously tapered resistive loading measures fast, time-varying, transient fields with minimal pulse-shape distortion due to nonlinear amplitude or phase characteristics of the transfer function. Although the antenna described in this paper was designed for a particular application, the theoretical design technique presented indicates that the approach can be used in other applications if extremely wide bandwidth and extremely low reflection coefficients are required.

## References

- [1] Kanda, M., The characteristics of a relatively short, broadband linear antenna with tapered resistive loading, International Symposium on Antennas and Propagation, Digest, 230-233, Stanford Univ., CA (June 1977).
- [2] Kanda, M., A relatively short, cylindrical broadband antenna with tapered resistive loading for picosecond pulse measurement, IEEE Trans. Antennas Propagat. AP-26, No. 3, 439-447 (May 1978).
- [3] Harrington, R. E., Field Computation by Moment Methods (New York: The MacMillan Company, 1968).
- [4] Wilton, D., Digest of numerical and asymptotic techniques for electromagnetics and antennas, University of New Mexico (March 1978).
- [5] Wu, T. T., and King, R. W. P., The cylindrical antenna with nonreflecting resistive loading, IEEE Trans. Antennas Propagat. AP-13, No. 3, 369-373 (May 1965).
- [6] Shen, L. C., and Wu, T. T., Cylindrical antenna with tapered resistive loading, Radio Science 2, No. 2, 191-201 (Feb. 1967).
- [7] Taylor, C. D., Cylindrical transmitting antenna: Tapered resistivity and multiple impedance loading, IEEE Trans. Antennas Propagat. AP-16, No. 2, 176-179 (March 1968).
- [8] Baum, C. E., Resistively loaded radiating dipole based on a transmission line model for the antenna, AFWL EMP1-6, 6, SSN-81, 1-27 (1970).
- [9] Kanda, M., Transients in resistively loaded antennas and their comparison with conical antennas and TEM horns, International Symposium on Antennas and Propagation, Digest, 13-16, Univ. of Maryland, MD (May 1978).
- [10] Kanda, M., Transients in resistively loaded antennas and their comparison with conical antennas and TEM horns, NBSIR 78-876, National Bureau of Standards, Boulder, CO (March 1978).
- [11] Harrington, R. F., Time-Harmonic Electromagnetic Fields (McGraw-Hill Book Co., 1961).
- [12] Harrison, C. W., Jr., and Williams, C. S., Jr., Transients in wide-angle conical antennas, IEEE Trans. Antennas Propagat. AP-13, 236-246, (March 1965).
- [13] King, R. W. P., The Theory of Linear Antennas (Harvard University Press, Massachusetts, 1956).

## Figure Captions

- Fig. 1 One-dimensional model for a resistively loaded "TEM" horn.
- Fig. 2 Biconical model for a conductive TEM horn.
- Fig. 3 Resistively loaded "TEM" horn.
- Fig. 4 Current distribution of a resistively loaded "TEM" horn.
- Fig. 5 Driving point impedance of a resistively loaded "TEM" horn:  
(a) Resistance;  
(b) Reactance.
- Fig. 6 Reflection coefficient of a resistively loaded "TEM" horn.
- Fig. 7 Reflection coefficients of various TEM horns.
- Fig. 8 Geometry for a resistively loaded "TEM" horn.
- Fig. 9 Radiation power patterns in the E plane.
- Fig.10 Radiation power patterns in the H plane.
- Fig.11 Transfer function of a resistively loaded "TEM" horn.
- Fig.12 Transfer function of a conductive TEM horn.
- Fig.13 Time-domain measurement:  
(a) Time-domain picosecond impulse;  
(b) Spectrum amplitude of picosecond pulse.
- Fig.14 Time-domain response of a resistively loaded "TEM" horn.

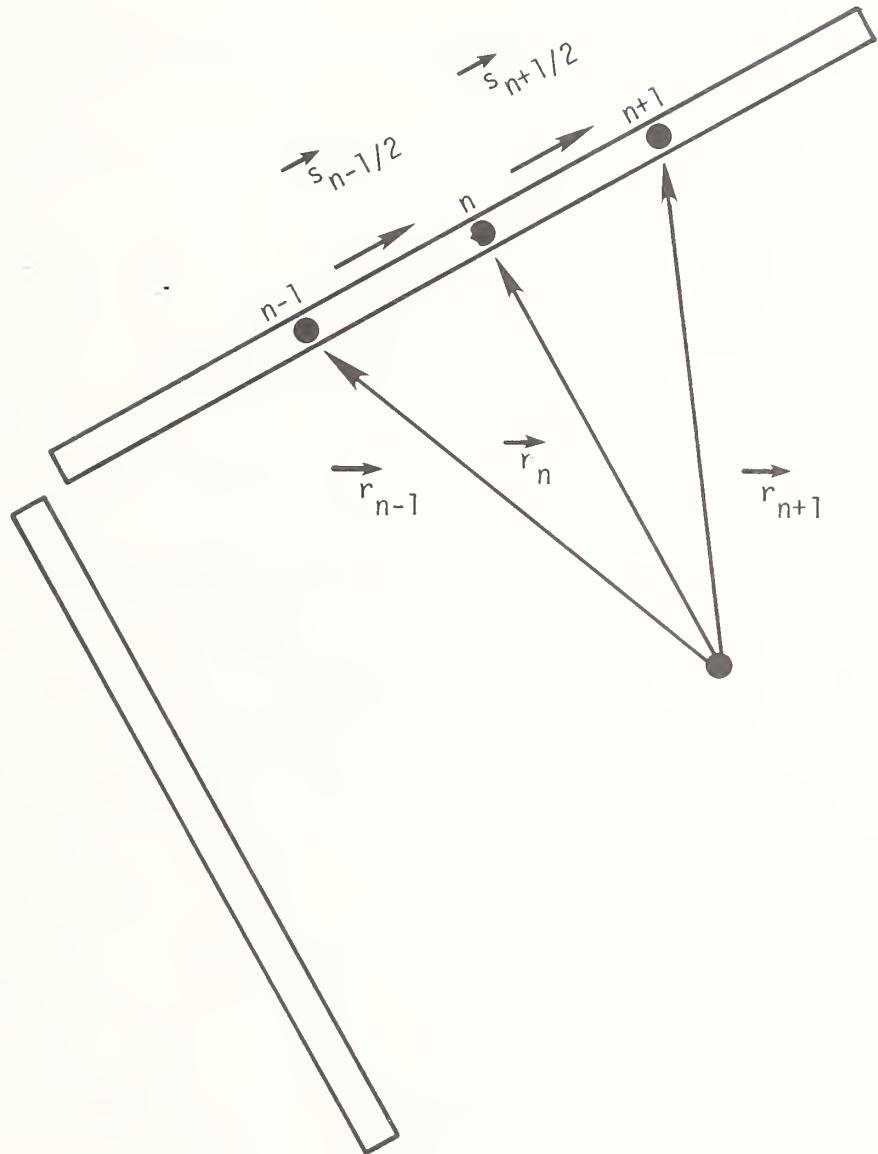


Fig. 1 One-dimensional model for a resistively loaded "TEM" horn.

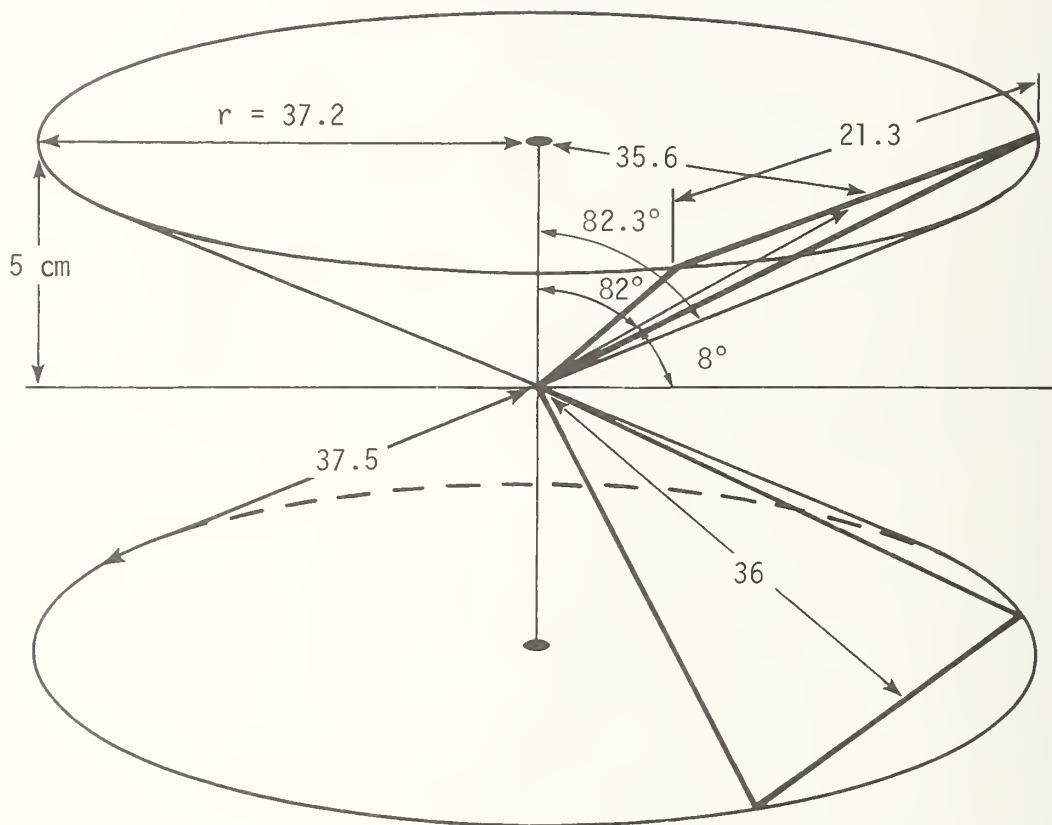


Fig. 2 Biconical model for a conductive TEM horn.

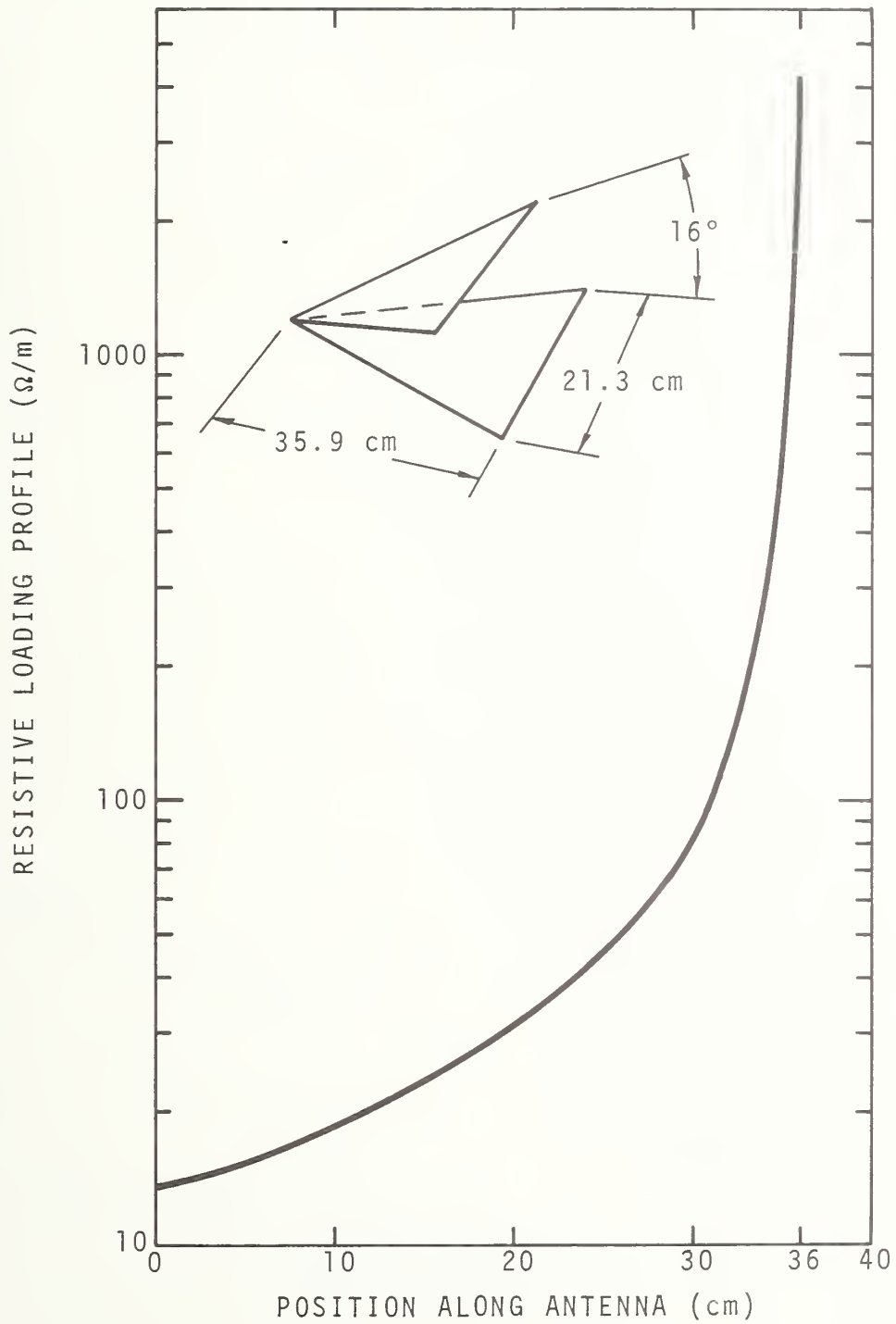


Fig. 3 Resistively loaded "TEM" horn.

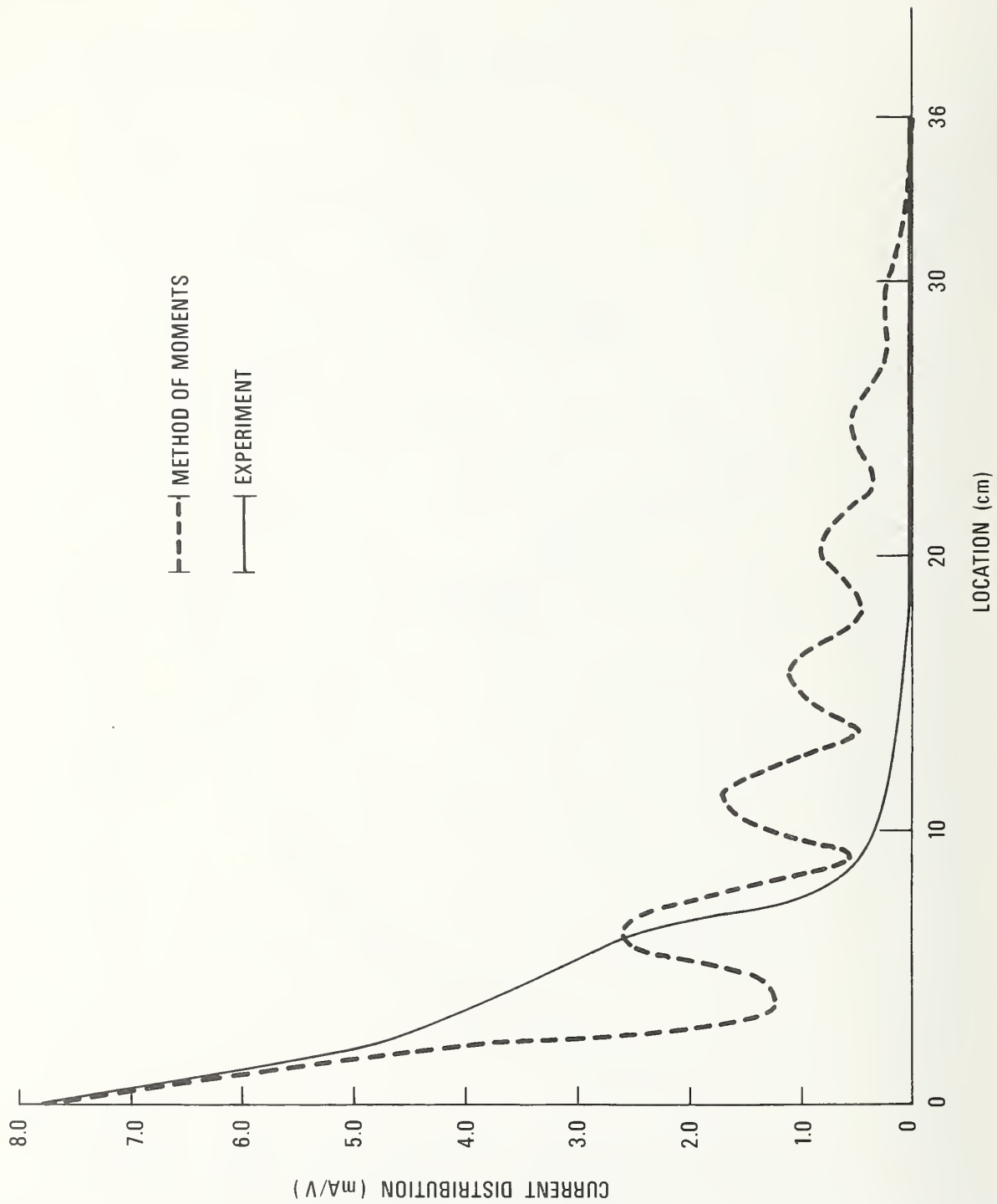
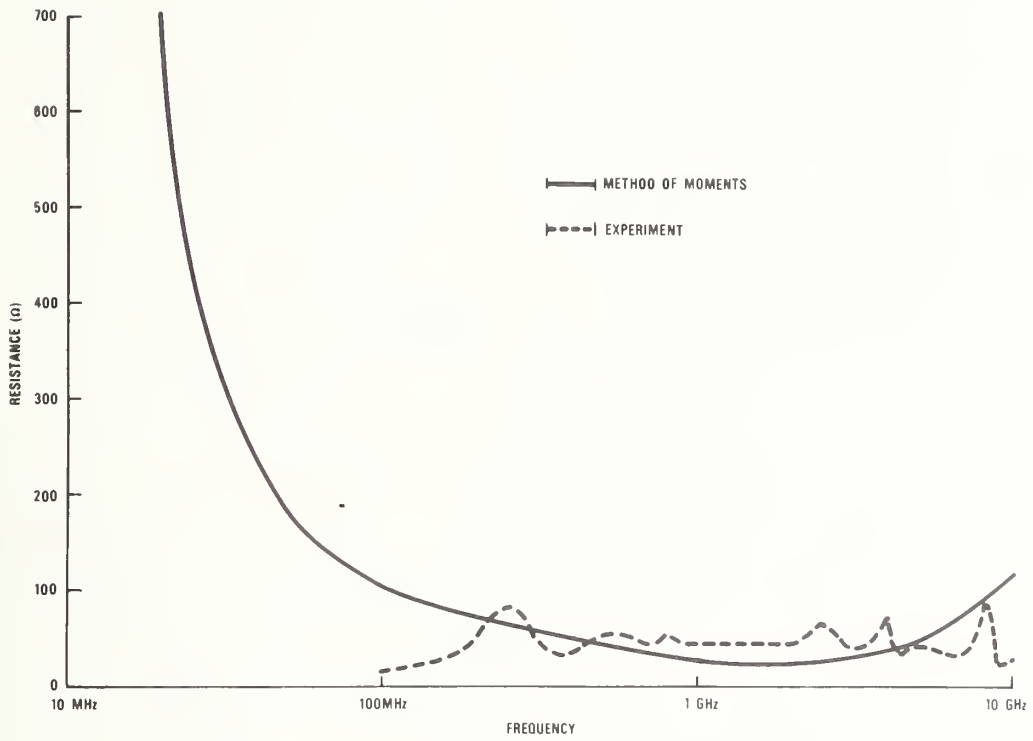
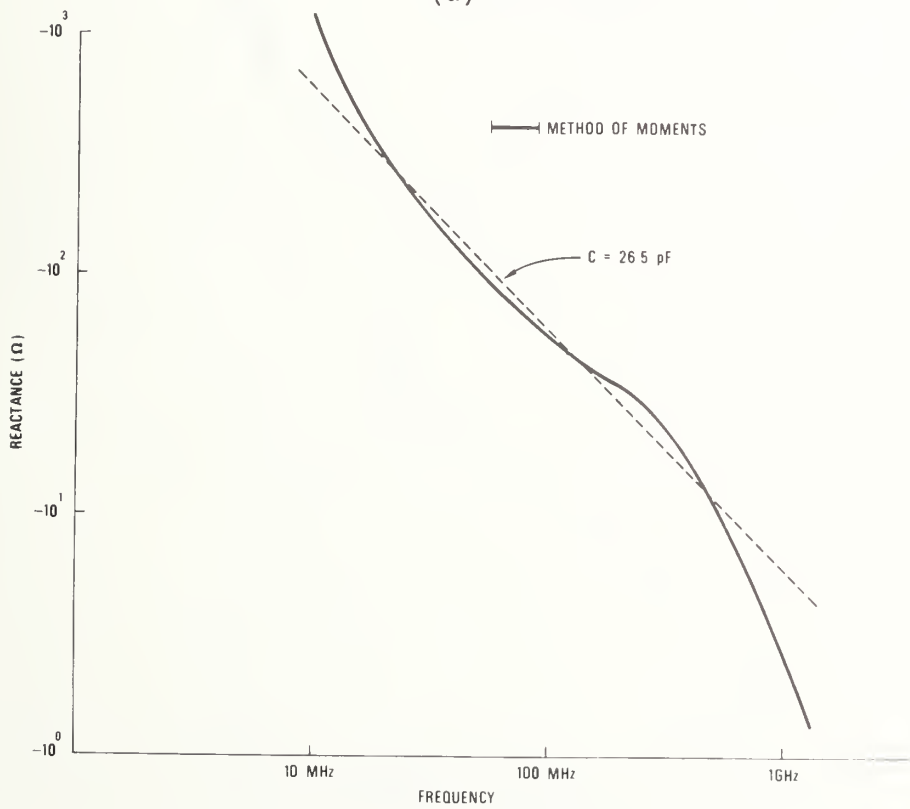


Fig. 4 Current distribution of a resistively loaded "TEM" horn.



(a) Resistance



(b) Reactance

Fig. 5 Driving point impedance of a resistively loaded "TEM" horn.

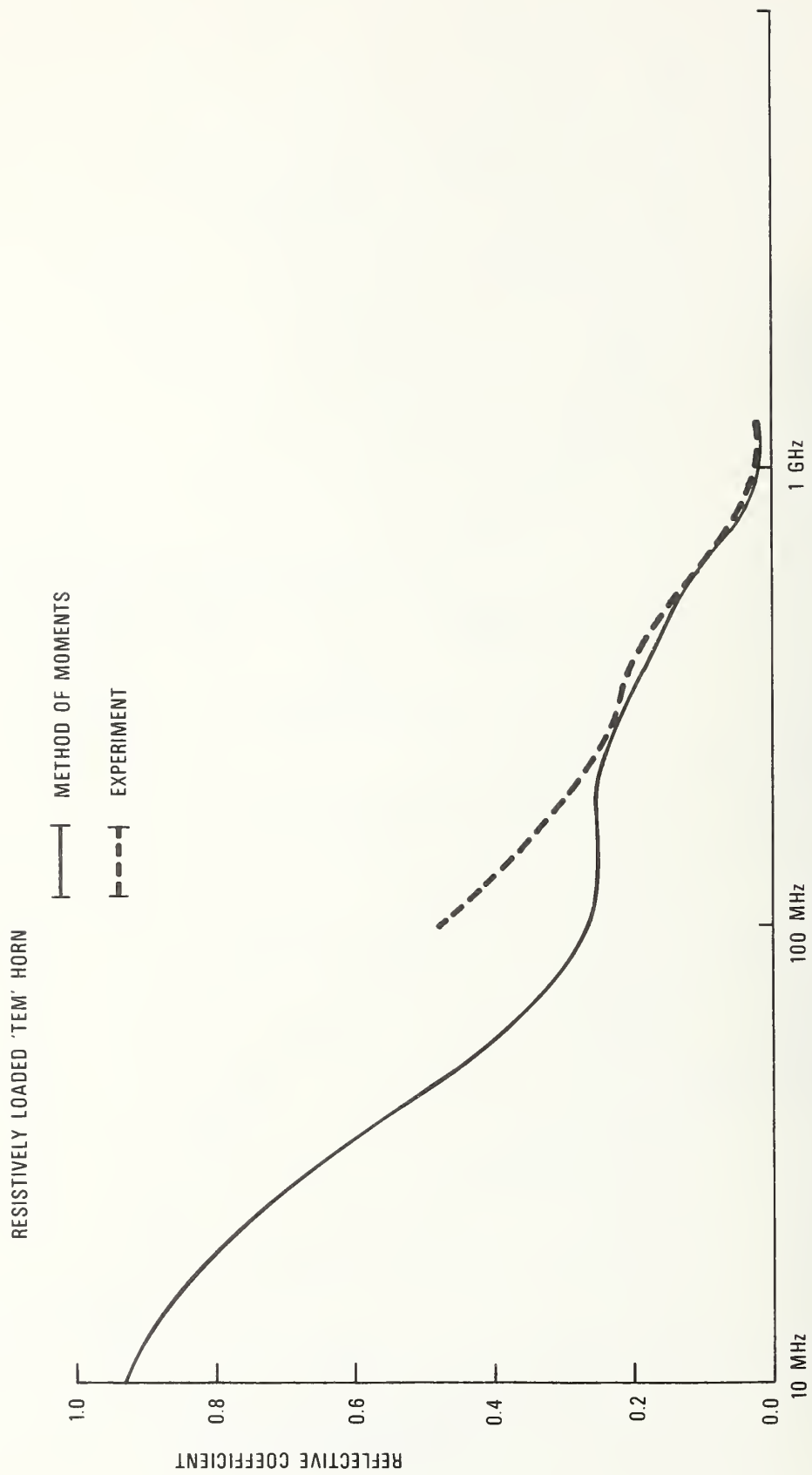


Fig. 6 Reflection coefficient of a resistively loaded "TEM" horn.

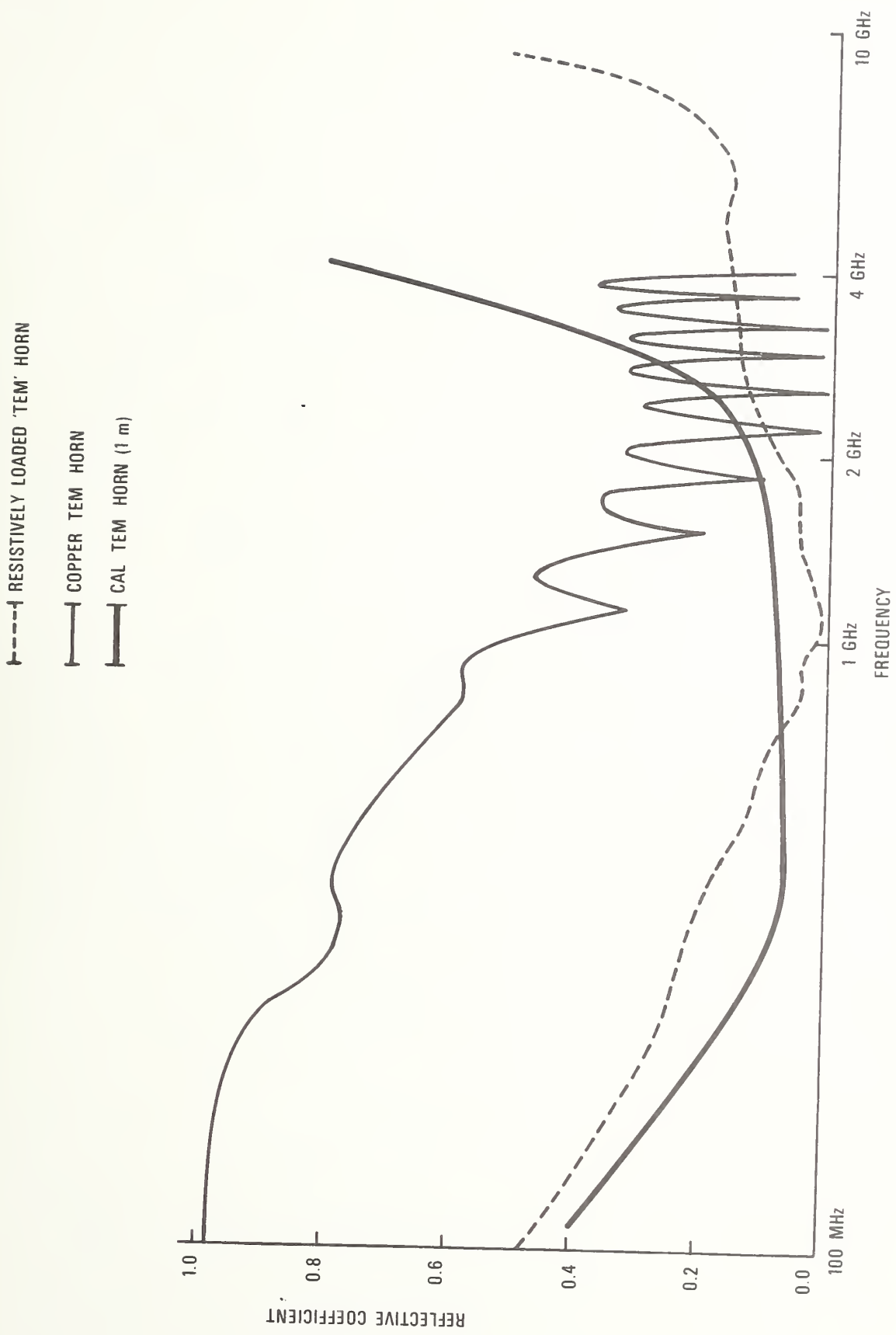


Fig. 7 Reflection coefficients of various TEM horns.

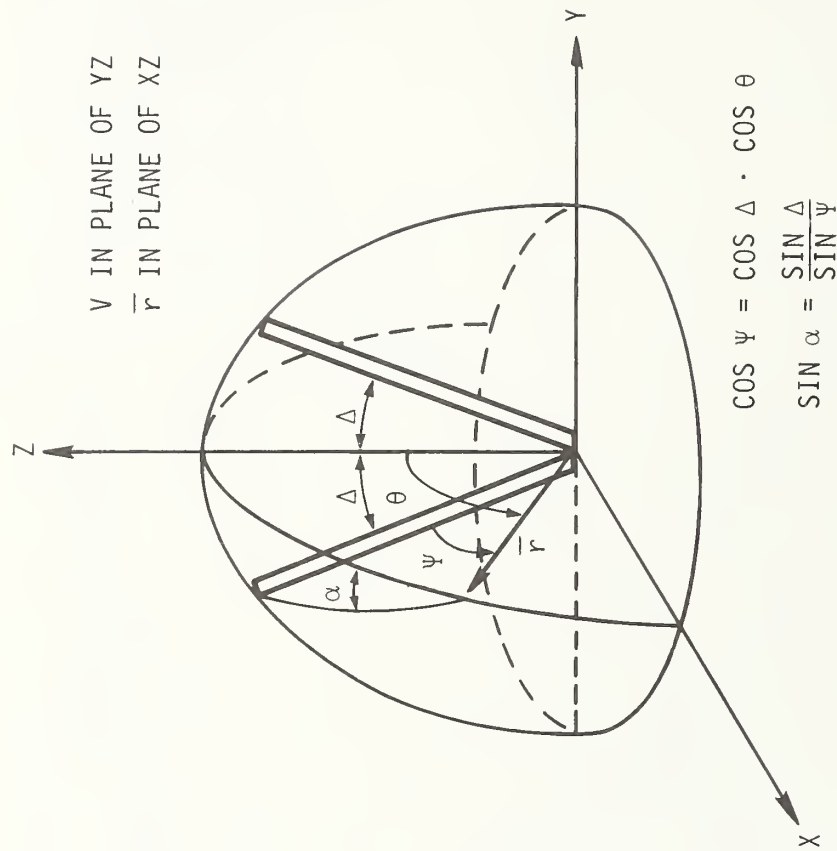


Fig. 8 Geometry for a resistively loaded "TEM" horn.

E PLANE PATTERN  
1 GHz

— THEORY

- - - EXPERIMENT

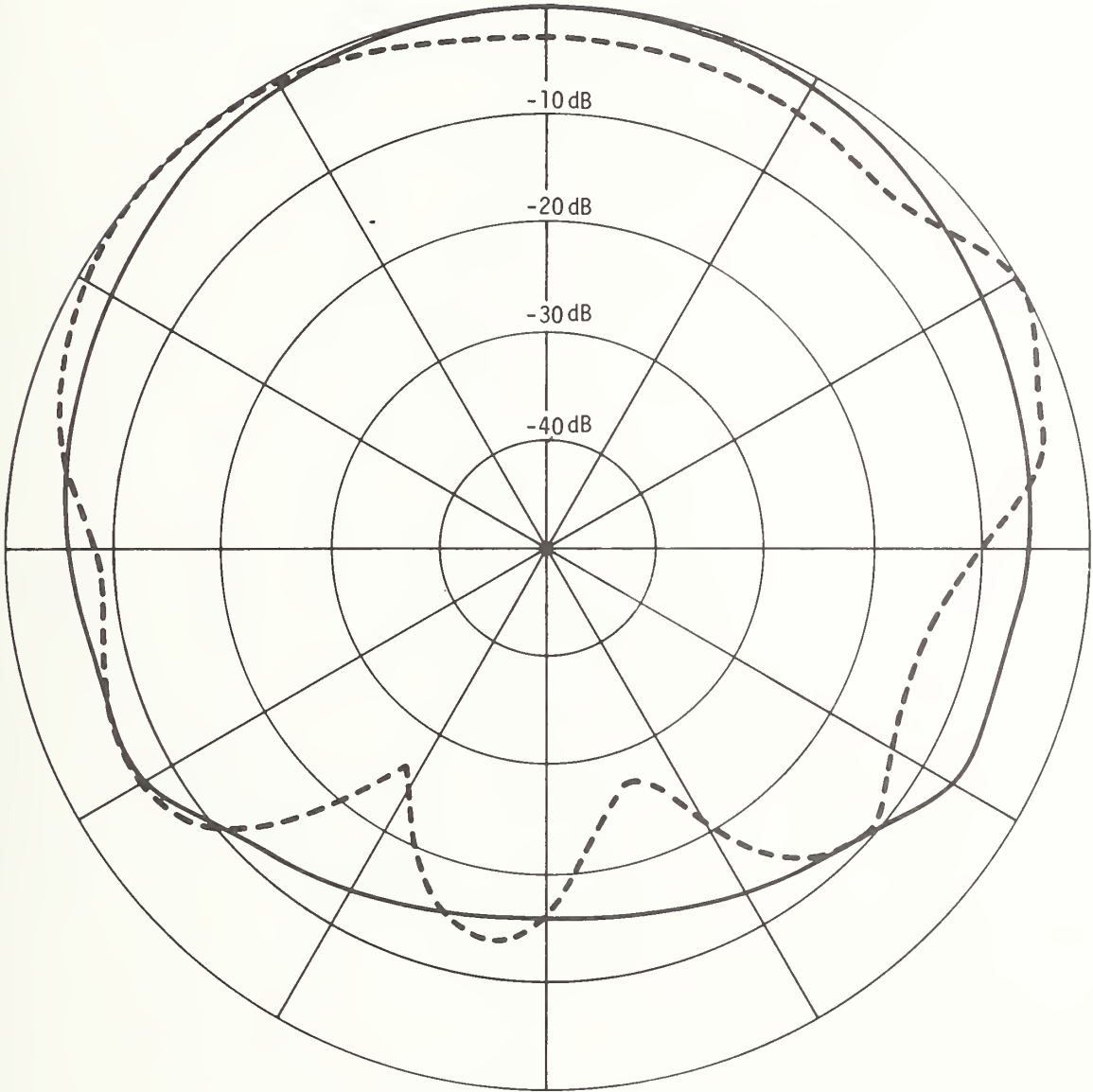


Fig. 9 Radiation power patterns in the E plane.

H PLANE PATTERN  
1 GHz

— THEORY  
- - - EXPERIMENT

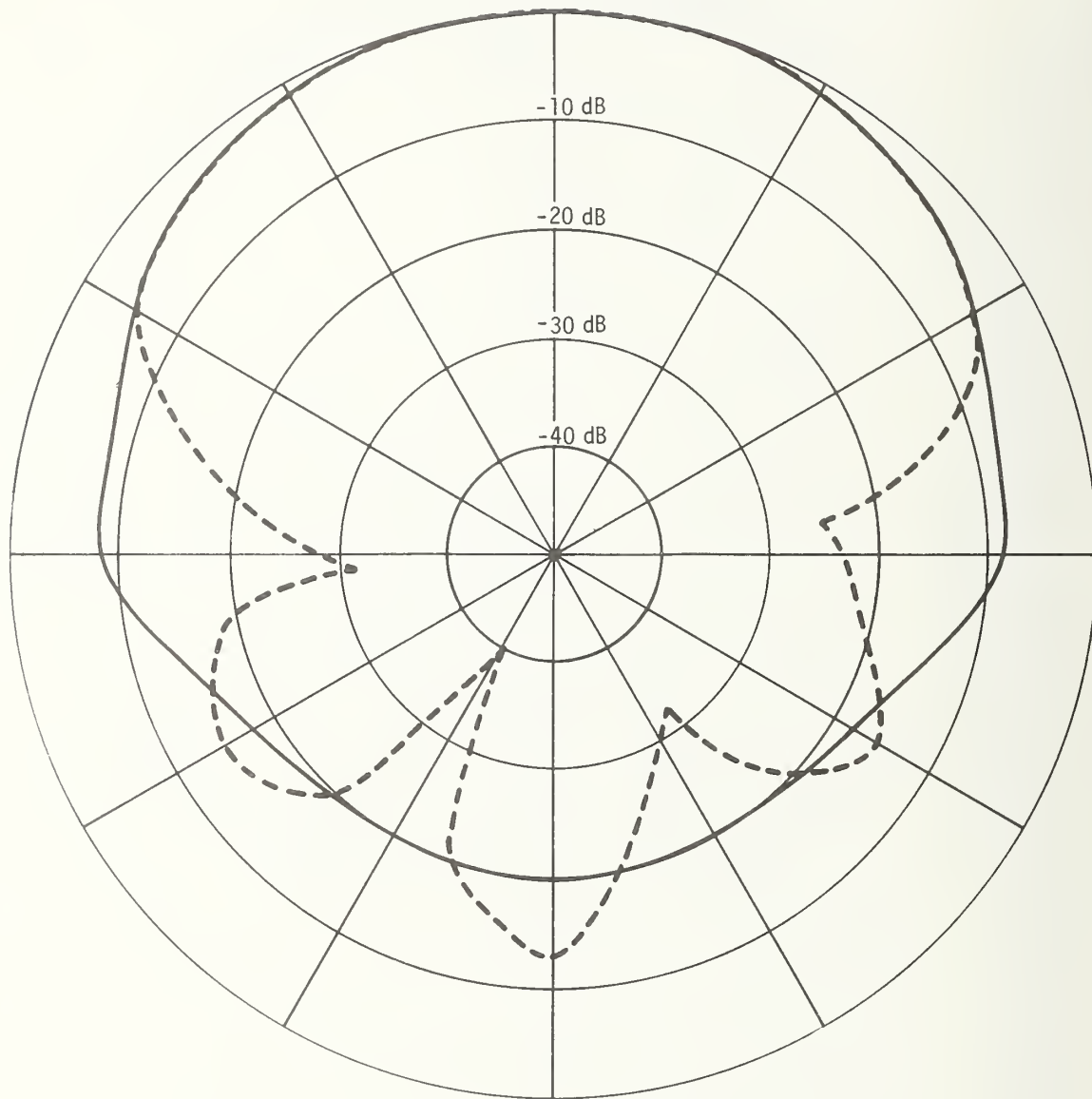


Fig.10 Radiation power patterns in the H plane.

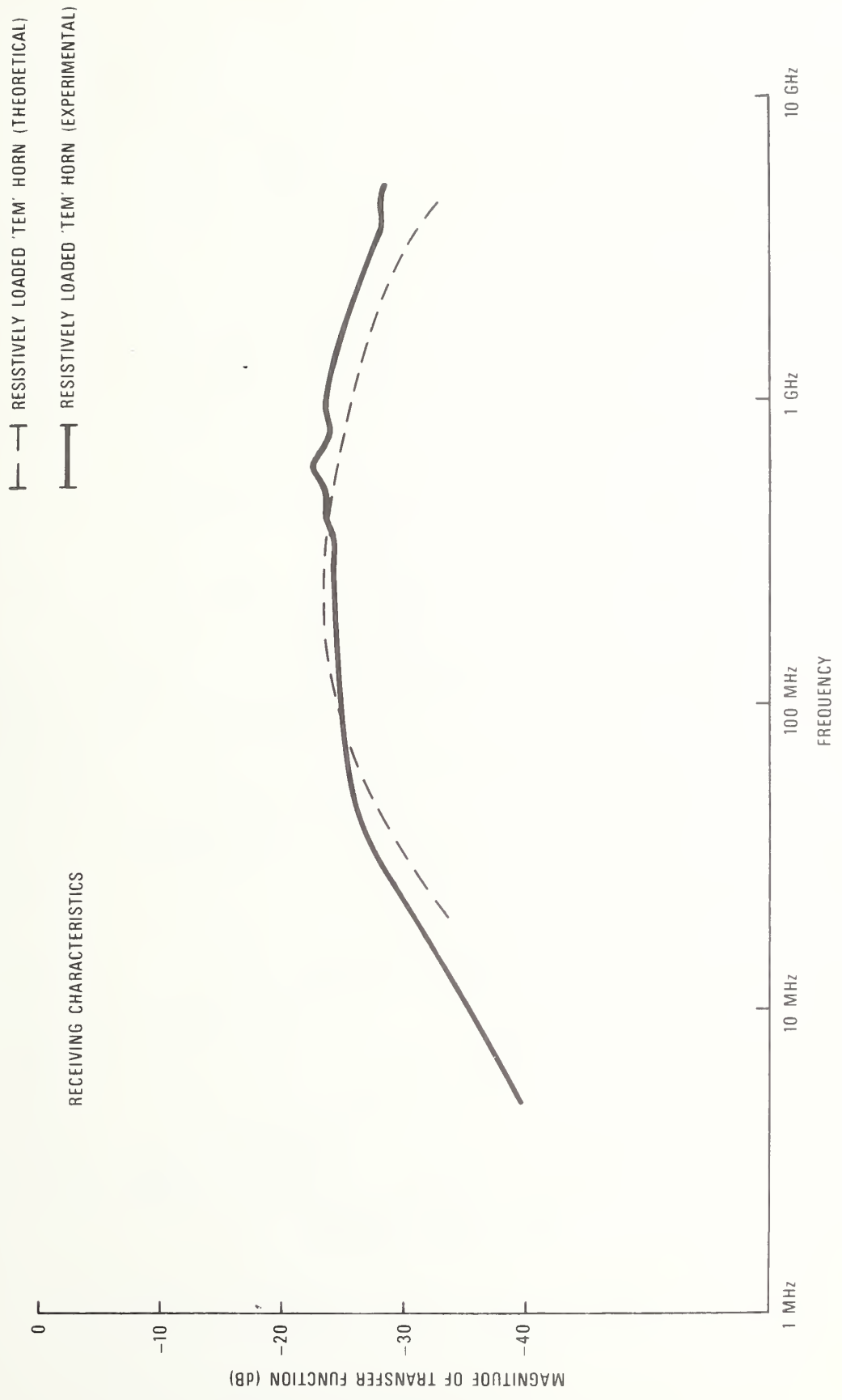


Fig.11 Transfer function of a resistively loaded "TEM" horn.

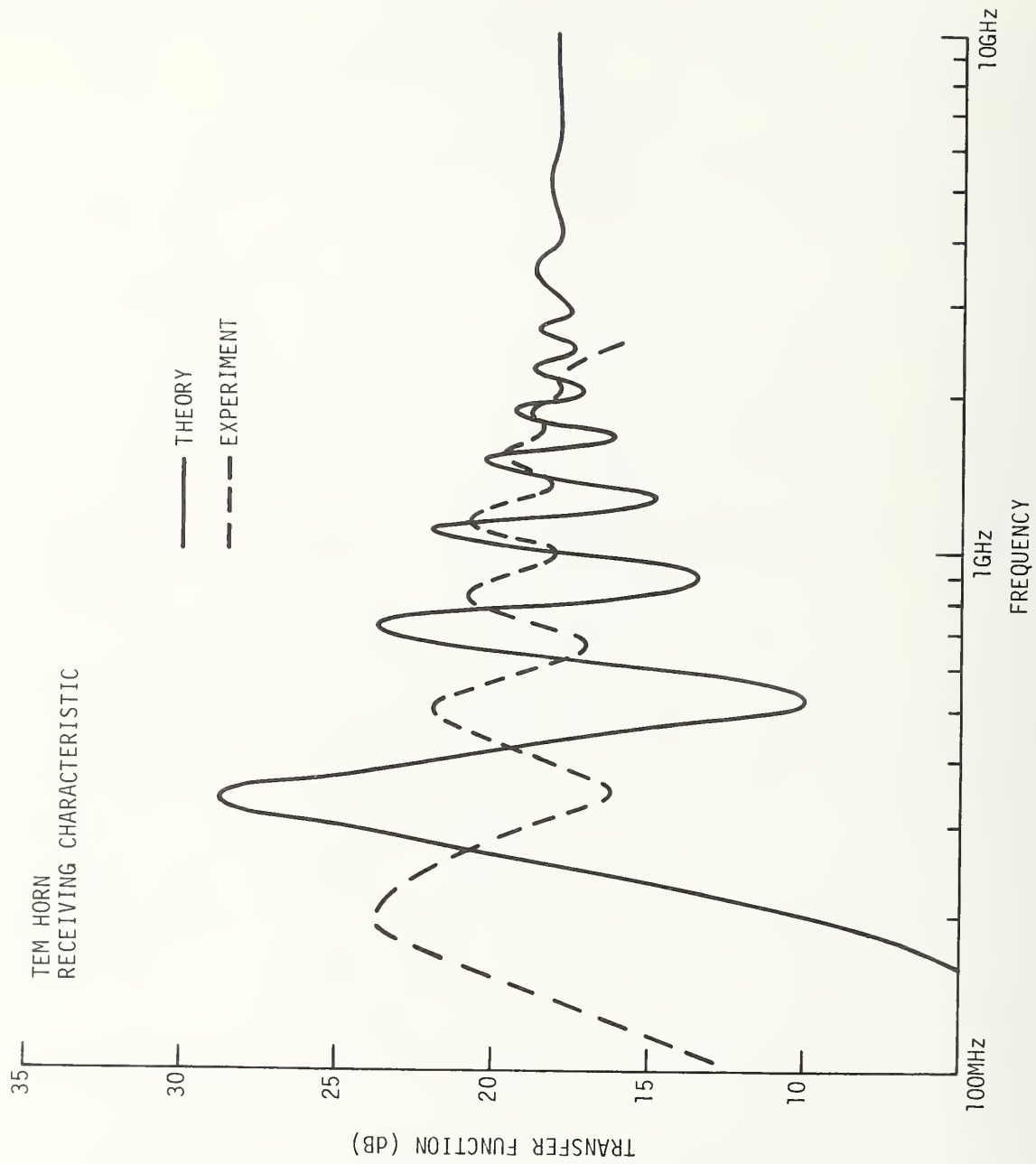
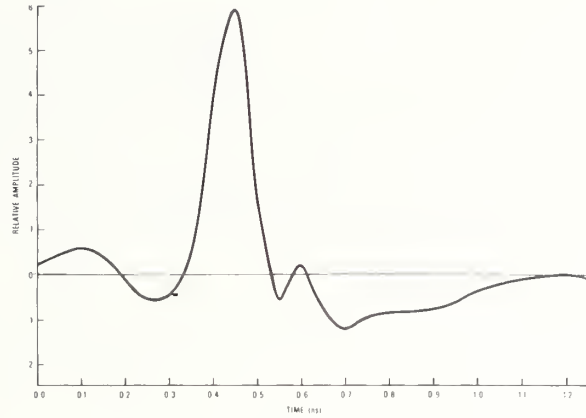
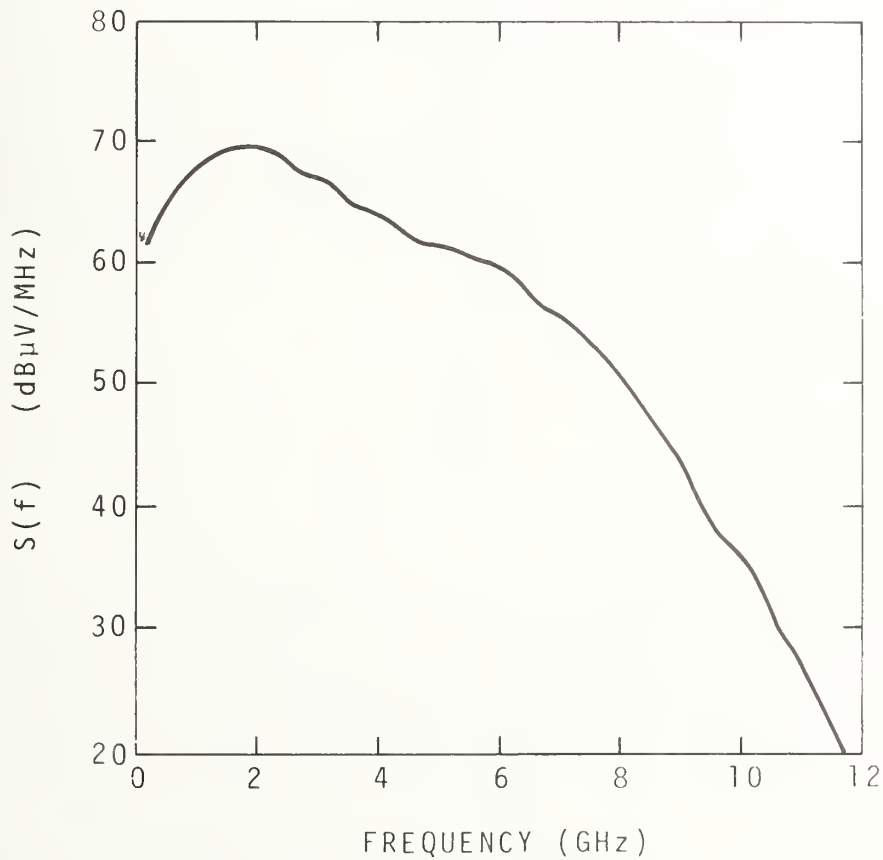


Fig.12 Transfer function of a conductive TEM horn.



(a) Time-domain picosecond impulse



(b) Spectrum amplitude of picosecond pulse

Fig.13 Time-domain measurement.

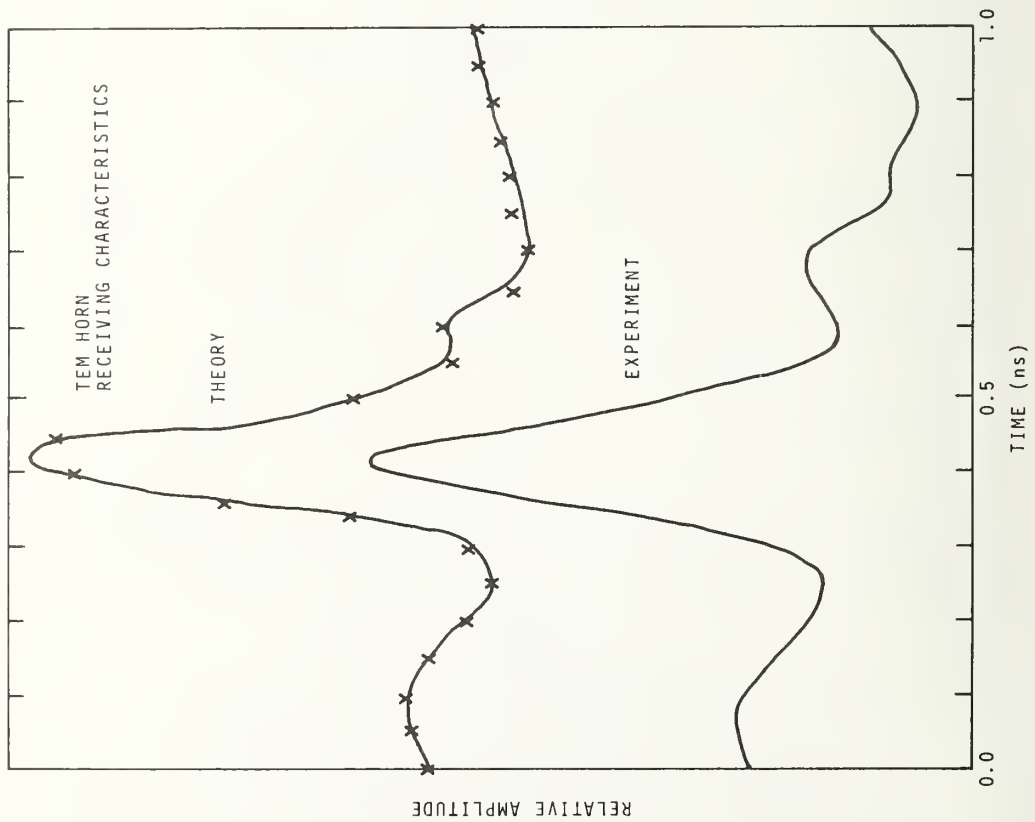
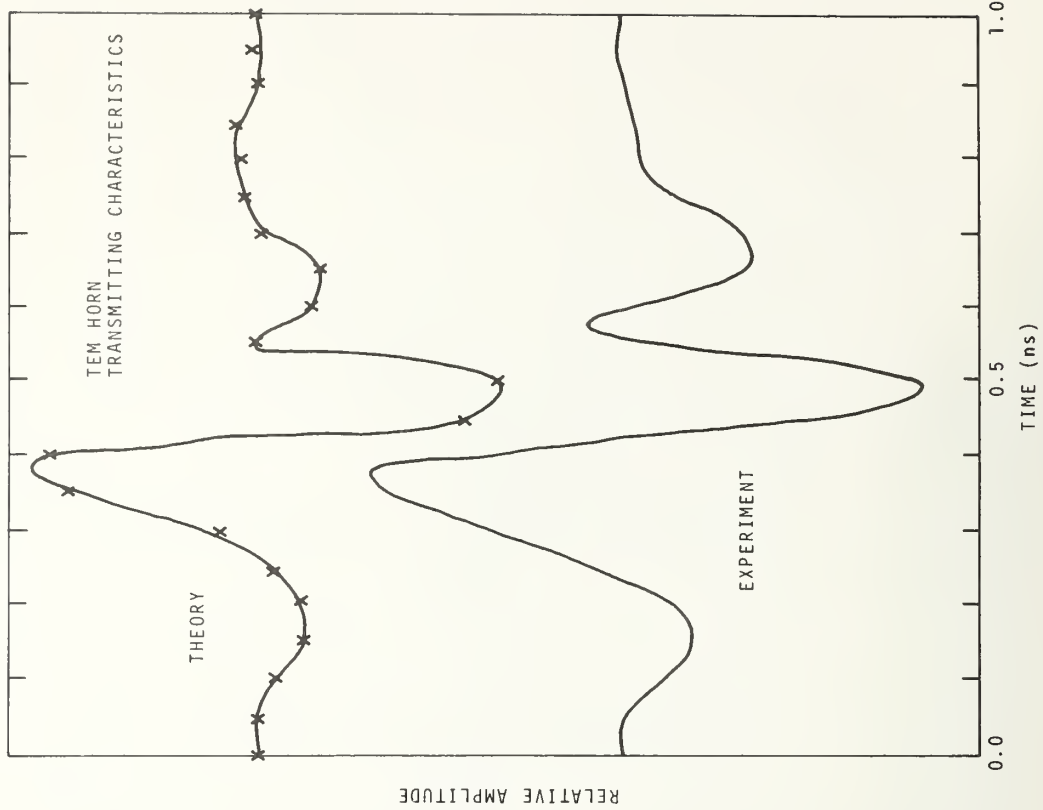


Fig.14 Time-domain response of a resistively loaded "TEM" horn.

U.S. DEPT. OF COMM. <b>BIBLIOGRAPHIC DATA SHEET</b>		PUBLICATION OR REPORT NO. NBSIR 79-1601	2. Gov. No.	Accession	3. Recipient's Accession No.
4. TITLE AND SUBTITLE  The Effects of Resistive Loading on TEM Horns			5. Publication Date August 1979		6. Performing Organization Code 723.03
			8. Performing Organ. Report No.		
7. AUTHOR(S) Motohisa Kanda			10. Project/Task/Work Unit No. 7233281		11. Contract/Grant No.
9. PERFORMING ORGANIZATION NAME AND ADDRESS  NATIONAL BUREAU OF STANDARDS DEPARTMENT OF COMMERCE WASHINGTON, D.C. 20234			13. Type of Report & Period Covered		
12. Sponsoring Organization Name and Complete Address (Street, City, State, ZIP)			14. Sponsoring Agency Code		
			15. SUPPLEMENTARY NOTES		
16. ABSTRACT (A 200-word or less factual summary of most significant information. If document includes a significant bibliography or literature survey, mention it here.)  For directional reception or transmission of picosecond pulses with minimal distortion, a short transverse electromagnetic (TEM) horn with continuously tapered resistive loading was developed, and found to be broadband and nondispersive with a low VSWR. The receiving transient response of the resistively loaded "TEM" horn indicates that the shape of 70-ps impulse is well preserved. The theoretical analyses using the method of moments and the fast Fourier transform (FFT) technique were performed and agreed well with time domain measurements.					
17. KEY WORDS (six to twelve entries; alphabetical order; capitalize only the first letter of the first key word unless a proper name; separated by semicolons)      Broadband; directivity; effective length; FFT; method of moments; nondispersive; picosecond pulse; resistive loading; TEM horn; transfer function; transient.					
18. AVAILABILITY  <input checked="" type="checkbox"/> For Official Distribution. Do Not Release to NTIS  <input type="checkbox"/> Order From Sup. of Doc., U.S. Government Printing Office Washington, D.C. 20402, SD Stock No. SN003-003  <input type="checkbox"/> Order From National Technical Information Service (NTIS) Springfield, Virginia 22161		19. SECURITY CLASS (THIS REPORT)  UNCLASSIFIED		21. NO. OF PAGES	
		20. SECURITY CLASS (THIS PAGE)  UNCLASSIFIED		22. Price	





